ResearchGate

See discussions, stats, and author profiles for this publication at: https://www.researchgate.net/publication/354922307

Measuring Irradiance for Bifacial PV Systems

Conference Paper · June 2021

DOI: 10.1109/PVSC43889.2021.9518601

CITATIONS
11

READS
704

10 authors, including:



Michael Gostein
Atonometrics
72 PUBLICATIONS **1,156** CITATIONS
SEE PROFILE



Silvana Ovaitt
National Renewable Energy Laboratory
36 PUBLICATIONS **367** CITATIONS
SEE PROFILE



Chris Deline
National Renewable Energy Laboratory
119 PUBLICATIONS **2,942** CITATIONS
SEE PROFILE

Aron Habte
National Renewable Energy Laboratory
117 PUBLICATIONS **1,792** CITATIONS
SEE PROFILE

Some of the authors of this publication are also working on these related projects:

Project
A Special Issue of Energies (ISSN 1996-1073, IF 2.707) on "Increasing the Lifetime of Photovoltaics Systems: Advanced Materials, Monitoring, O&M and Energy Modeling" View project

Project
IEA PVPS Task 16: Solar resource for high penetration and large scale applications View project

All content following this page was uploaded by Michael Gostein on 29 September 2021.

The user has requested enhancement of the downloaded file.

Measuring Irradiance for Bifacial PV Systems

Michael Gostein[1], Silvana Ayala Pelaez[2], Chris Deline[2], Aron Habte[2], Clifford W. Hansen[3], Bill Marion[2], Jeff Newmiller[4], Manajit Sengupta[2], Joshua S. Stein[3], Itai Suez[5]

[1]Atonometrics, Austin, TX, 78757, USA; [2]National Renewable Energy Laboratory, Golden, CO, 80401, USA; [3]Sandia National Laboratories, Albuquerque, NM, 87123, USA; [4]DNV, Oakland, CA, 94612, USA; [5]Silfab Solar, Mississauga, ON, L5T2Y3, Canada

***Abstract* — The advent of bifacial PV systems drives new requirements for irradiance measurement at PV projects for monitoring and assessment purposes. While there are several approaches, there is still no uniform guidance for what irradiance parameters to measure and for the optimal selection and placement of irradiance sensors at bifacial arrays. Standards are emerging to address these topics but are not yet available. In this paper we review approaches to bifacial irradiance monitoring which are being discussed in the research literature and pursued in early systems, to provide a preliminary guide and framework for developers planning bifacial projects.**

***Index Terms* — photovoltaic systems, bifacial, irradiance measurement, performance analysis, solar energy**

I. Introduction

With the adoption of bifacial modules in PV systems, developers of PV power plants face new challenges in deciding how best to measure irradiance for system monitoring and assessment against performance guarantees. There is a growing body of work examining methods for standardizing power output measurements of bifacial PV modules and predicting bifacial PV array performance under given conditions of front and rear irradiance, primarily as an aid to system design [1][2][3][4][5][6]. However, for the construction of new PV power plants employing bifacial modules, there is still no uniform guidance on the type, quantity, and placement of irradiance sensors in a monitoring system or for the use of irradiance data for monitoring and assessment in performance contracts.

Standards are emerging to address these topics. IEC 61724-1, which covers PV system performance monitoring, is currently undergoing revision to Edition 2. A major new component of this revision is the addition of requirements and recommendations for irradiance measurement in bifacial systems. The draft document also includes definitions of metrics for bifacial systems. In other work, proposals for adapting PV system capacity testing to bifacial systems have been explored [7]. A new effort is currently underway to update IEC 61724-2 and IEC 61724-3, which cover capacity and energy testing, for the bifacial era.

In this paper we will provide a review of various options and recommendations for bifacial system irradiance monitoring which are being discussed in the research literature as well as the international standards development community, while being pursued in practice on early adopters' and prototype research and development systems. The intent of this work is to provide a preliminary guide and framework for discussion to assist researchers, owner's engineers, and developers that are actively planning projects.

II. Challenges

A. Overview

Ultimately the goal of measuring or modeling both the front and rear-side irradiance of a bifacial PV system is to arrive at a time-dependent value of the solar resource which can be used to predict PV system power output and/or ensure that the system is functioning as intended.

Irradiance reaching the front-side and rear-side plane-of-array (POA) of bifacial PV modules includes many components, as illustrated in Fig. 1. These include direct radiation from the sun, diffuse radiation from the sky, and ground-reflected radiation. These components have different relative contributions on the front and rear sides of bifacial modules.

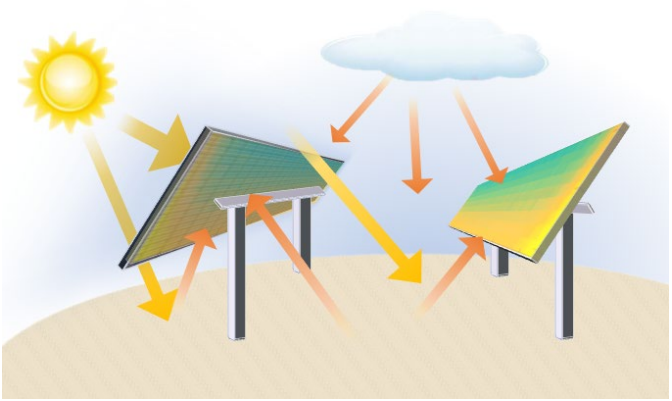


Fig. 1. Contributions to illumination of front and rear of bifacial PV modules, including direct, diffuse, and ground-reflected radiation.

Sandia National Laboratories is a multimission laboratory managed and operated by National Technology and Engineering Solutions of Sandia, LLC, a wholly owned subsidiary of Honeywell International Inc., for the U.S. Department of Energy's National Nuclear Security Administration under contract DE-NA0003525.

This work was supported by the U.S. Department of Energy under Contract No. DE-AC36-08-GO28308 with the National Renewable Energy Laboratory (NREL). Funding provided by the U.S. Department of Energy's Office of Energy Efficiency and Renewable Energy (EERE) under Solar Energy Technologies Office (SETO) Agreement Number 34910.

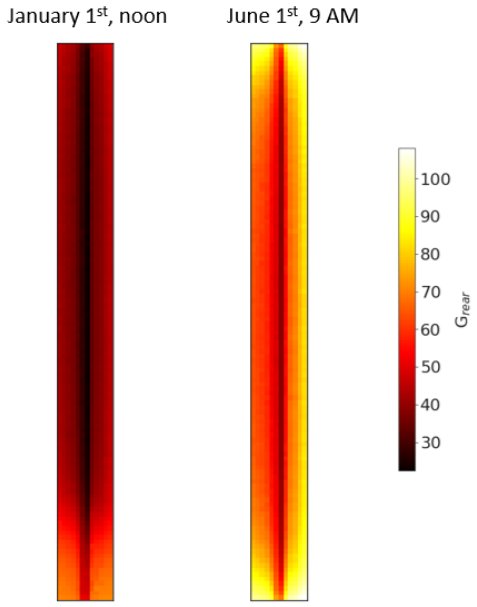


Fig. 2: Modeled rear irradiance for each cell in a single-axis tracker row at the center of a 7-row x 20-module array. Modeled for January 1st at noon and June 1st at 9 am in sunny conditions at Golden, CO. Non-uniformities are seen both near the row edges and across the collection width perpendicular to the row. Irradiance scale is in W/m^2. Rows are north-south.

While methods of front-side irradiance measurements for monitoring the performance of monofacial solar PV systems are already well established, for bifacial systems industry consensus on measurement methods has not yet been reached. There are multiple challenges to consider. These include spatial and time-varying non-uniformity of rear-side irradiance, the relative impact of diffuse versus direct radiation, uncertainty in ground reflection, and spectral effects. System design parameters affecting these uncertainties include ground clearance height, view factor, ground coverage ratio, tracking, rear-side shading caused by racking components such as torque tubes and rails, and variability in the reflective properties of the ground surface due to angular and spectral dependencies. Choices of the sensor types, locations, and quantities in combination with the unique parameters of the design itself will define how much uncertainty will exist in the assessment of a bifacial system's performance.

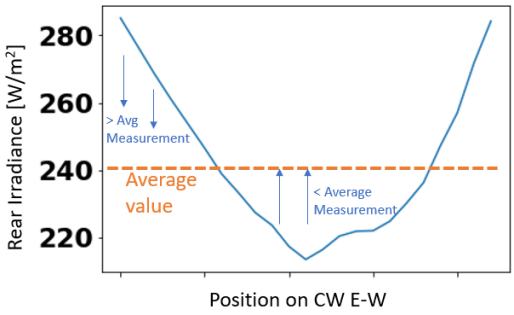


Fig. 3. Rear-side irradiance versus east-west position across north-south oriented module rows, showing irradiance non-uniformity. Adapted from [4].

B. *Non-uniformity*

The non-uniformity of rear-side irradiance and its impact on power generation are especially significant factors affecting both measurement and modeling, increasing uncertainty in performance prediction.

Fig. 2 illustrates some key aspects of rear-side irradiance non-uniformity, using a simulation of rear-side irradiance for each cell in 20-module row at the center of a 7-row single-axis tracking array. Simulations are performed for sunny conditions in Golden, Colorado, for two different days and times. Both simulations show irradiance at the row-ends of only ~50-75% that at the row-center as well as significant transverse non-uniformity and torque-tube shading along the center line. The irradiance profile will change throughout the day: note in the 9 am simulation the enhanced irradiance on the eastern side towards the morning sun. The changing non-uniformity patterns displayed in Fig. 2 complicate the potential placement of rear-side irradiance sensors, since no single sensor location represents conditions along the entire row.

Some modeling software packages simplify the rear-side non-uniformity by predicting only an average rear-side irradiance value. However, Fig. 3 shows an example of how

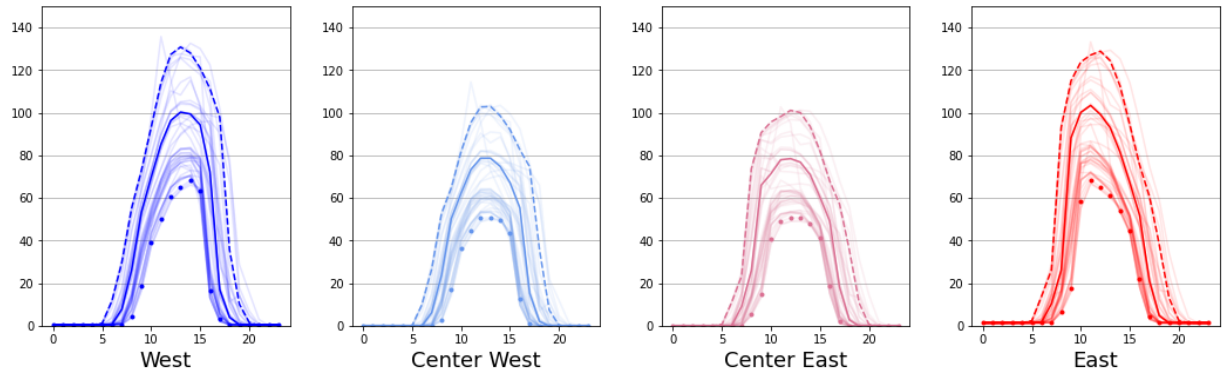


Fig. 4: Measured non-uniformity of rear irradiance, showing spatial, temporal, and seasonal changes. Four rear-facing reference cells along collector width of row (West to East) indicate lower rear irradiance values (y-axis, W/m^2) in the center (Center-West, Center-East) than the edges (West, East), with hour-of-day (x-axis) variation and seasonal variation (dashes = July 1, solid = September 1, dotted = December 25, faint lines = selected clear sky days in 2020).

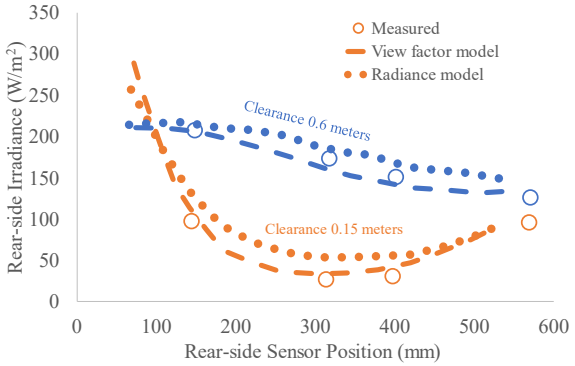


Fig. 5: Rear-side irradiance non-uniformity is reduced as ground clearance height is increased. The figure compares measurements, view factor model, and Radiance model for irradiance transverse to a module row.

much the actual irradiance across the rear side of bifacial modules can deviate from the average. In this example, for a single axis tracking system with modules on either side of a torque tube, the irradiance is approximately 20% lower near the center rotation axis than at the module edges.

Fig. 4 illustrates another example of rear-side irradiance spatial and temporal variability. In the example shown by the figure, rear-side irradiance measurements on a single axis tracking system show variability from one transverse edge of the modules to the other based on both time of day as well as day of year. The figure shows up to ~30% greater irradiance on the module edge towards the sun (east or west) during morning or afternoon, with this non-uniformity varying throughout the year.

Spatial non-uniformity is also a function of system design. Fig. 5 illustrates the impact of ground clearance height on the rear-side irradiance transverse to a module row, with higher clearance height leading to greater irradiance and significantly reduced non-uniformity – but also greater costs for racking.

C. *Diffuse fraction*

Diffuse light fraction adds another complication. In a simplistic assumption, average rear-side irradiance could be considered proportional to front-side irradiance; however, Fig. 6 shows that this assumption is incorrect. Each point in the plot is an hourly modeled spatially averaged irradiance combination comparing rear and front POA irradiance from a typical year of data for a horizontal single axis tracking array located in Wisconsin. The green and red circles represent data from days with high and low diffuse irradiance, respectively. Depending on whether the performance of this system is evaluated on days with high or low diffuse fraction, the proportionality of rear to front POA irradiance can vary on the order of a factor of up to 4, with higher diffuse fraction leading to relatively greater rear-side irradiance. Since this can correspond to deviations of 20% relative to a model that ignores rear POA, short-term performance evaluation methods should not neglect rear POA or diffuse fraction.

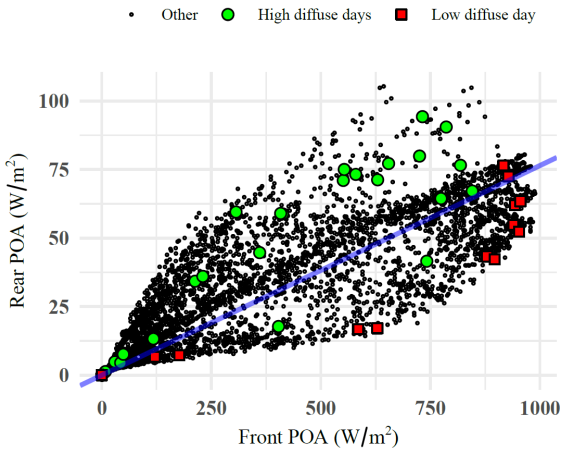


Fig. 6. Impact of different diffuse irradiance fraction conditions, showing non-proportionality of rear-side and front-side POA irradiance. Green: sample high diffuse fraction days. Red: sample low diffuse fraction days.

D. *Albedo*

Albedo, the reflectivity of the ground surface, is of course critical to bifacial PV system performance. The detailed angular and spectral distribution of ground-reflected radiation is complex [8][9]. However, as a simplification, most PV performance modeling software considers the albedo of a ground surface as a single number representing the ratio of total reflected light to total incident light.

For modeling bifacial systems, albedo values for ground surfaces similar to what is expected to be on site are often used. These values are often obtained from nearby weather stations with albedometers or from satellite sources [10][11][12]. In cases where no data are available, standard average values of albedo can be used [13]. Some weather files such as the National Solar Radiation Database [11] include albedo values to be used for generalized modeling. Data sets of ground albedo and associated meteorological data developed by using existing

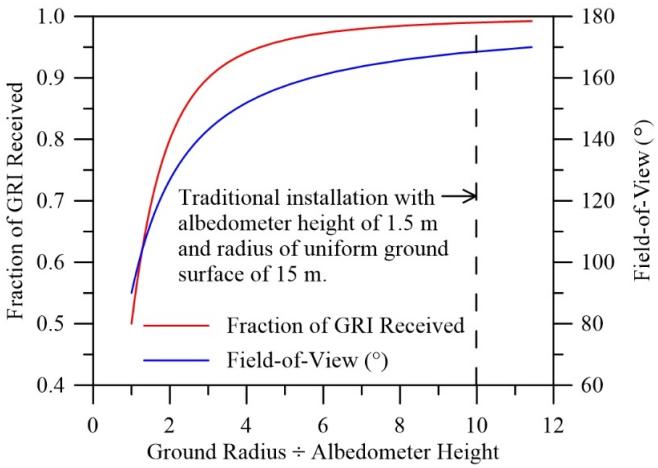


Fig. 7. Relationships between albedometer installation height, viewed ground radius, field of view, and the fraction of the ground-reflected irradiance (GRI) received by the albedometer.

measurement network data and data contributed by the PV industry are available for download from NREL's DuraMAT website at https://datahub.duramat.org/project/about/albedo-study [14]. The user's guide includes plots of monthly and hourly albedos to illustrate seasonal and diurnal variations in albedo for a location.

PV modeling software typically supports monthly values for albedo, which may change seasonally due to ground moisture content, snow, or changes in vegetation [8][9]. More detailed projections include hourly values and are often suggested to capture performance variations between low sun elevation angles and diffuse light conditions. Alternatively, long-term energy predictions may average over seasonal variations [15][16].

Albedo values used in modeling should be for identically prepared ground surfaces, including any dust mitigation schemes.

As a complication, during initial powering of a system the terrain will usually not reflect expected topography, for example due to trampled grass or moved flora or ground. Care should be taken to correct for the projections with on-site measurements at deployment. Afterwards, keeping albedometers on site is recommended for continued performance evaluation of the bifacial system.

Measuring on-site albedo is beneficial for bifacial systems performance evaluation. Installation of an albedometer requires a ground surface representative of the site and the appropriate size for the field of view of the albedometer. Fig. 7 illustrates the relationships between albedometer installation height, viewed ground radius, field of view, and the fraction of the ground-reflected irradiance (GRI) received by the albedometer for uniform isotropic reflection. For an albedometer installation height of 1.5 m and a manufacturer's recommendation that the viewed ground radius be 10 times the mounting height, the field of view is 170° and 99% of the GRI is received from within this field of view. IEC 61724-1 is less stringent with a ±80° or 160° field-of-view recommendation. Within this field-of-view, the albedometer would receive about 93% of the GRI and the viewed ground radius is reduced from 15 m to 8.3 m. A representative ground surface directly under the albedometer is also important because 50% of the GRI is received from within a ground radius equal to the mounting height.

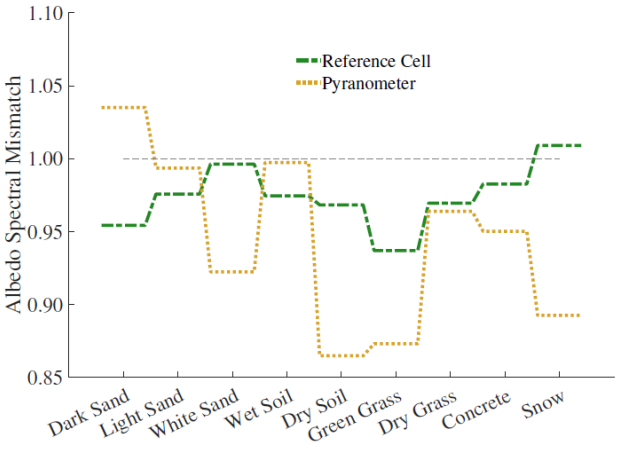


Fig. 8. Influence of spectral albedo. Variation in albedo spectral mismatch versus representative bifacial PV module, for PV reference cell and broadband pyranometer, over a range of ground surfaces. [19]

In some cases, ground surface may not be uniform within a region conveniently measured by an albedometer. This can occur for example in systems with albedo-boosting reflector materials, pavers, or fabrics; in built environments with complex structures, such as parking shade structures; or in emerging projects combining agricultural and PV land use. In these cases, one approach is to use an average value of albedo, perhaps derived from measurements on a grid.

E. Spectral response

The choice of irradiance sensor may have a significant effect on the determination of effective irradiance and the accuracy of performance predictions because of spectrally responsive albedo. Spectral reflection of ground surfaces can vary significantly [17], both from one surface to another and also seasonally due to variations in soil moisture content, vegetation, snow, and other factors. Therefore, measured rear irradiance with sensors with different spectral responsivities than PV devices can provide a range of results. At one site, measurements with broadband pyranometers showed a 20% higher response relative to reference cells for eight months of rear-irradiance measurements [18]. Simulations for a set of nine representative ground surfaces found that spectral mismatch relative to a bifacial module was distributed over a range of ±9.2% for thermopile pyranometers versus only ±3.7% for a typical PV reference cell [19], as shown in Fig. 8.

However, selection of broadband pyranometers versus reference cells may also be impacted by intended purpose. For validating rear-irradiance optical models which are spectrally agnostic, broadband sensor measurements show better model agreement [20]. However, for assessing rear-side contribution to module power production, reference cells provide a closer match to module performance because of their better spectral match [19].

In modeling, the effect of spectral mismatch effects on rear irradiance is still being evaluated. Furthermore, for bifacial tandem cells and modules, a better understanding of the front and rear spectral response is required [21].

III. Performance Equations

Existing methods and standards for plant performance assessment, such as capacity tests and performance ratios, need to be adapted to bifacial systems.

One approach to this adaptation, proposed for capacity tests in [7], is to modify traditional performance metrics for monofacial systems, replacing the in-plane front-side

irradiance G_{POA} with an effective irradiance G_{eff} which includes the contributions of both front- and rear-side POA irradiance to system power. This effective irradiance can be written

$$G_{eff} = G_{POA} + G_{rear} \cdot \varphi_{Pmax} \quad (1)$$

where G_{rear} is the rear-side plane-of-array irradiance and φ_{Pmax} is the bifaciality factor of maximum power defined in IEC 60904-1-2, the ratio between power produced by rear-side versus front-side irradiance contributions. The φ_{Pmax} term is obtained from PV module datasheets and should be measured according to IEC 60904-1-2 or similar methods.

The above definition is chosen to enable module power output to be written in terms of G_{eff} as

$$P = G_{eff} \cdot P_0 \cdot \left(1 + \gamma \cdot (T - T_0)\right) \quad (2)$$

where P_0 is the module's front-side power rating at the reference condition (e.g., STC), γ is the temperature coefficient of power, T is temperature, and T_0 is the reference temperature.

We use the term "effective" irradiance for G_{eff} because it is quantified in terms of its effect on total module power output, via eq. (2), and depends on module characteristics, via φ_{Pmax}, rather than on irradiance alone. Note that, more generally, eq. (1) could be elaborated to consider other characteristics that affect module power output, such as spectral and angular response, non-uniformity, structural shading, or electrical mismatch, by incorporating additional correction or mismatch factors in determination of effective irradiance, according to its impact in eq. (2).

The draft of IEC 61724-1 Edition 2 reorganizes eq. (1) in the algebraically equivalent form

$$G_{eff} = \left(1 + \varphi_{Pmax} \cdot \frac{G_{rear}}{G_{POA}}\right) \cdot G_{POA} \quad (3)$$

$$= BIF \cdot G_{POA} \quad (4)$$

to define the bifacial irradiance factor *BIF* representing the terms in parenthesis in eq. (3). Eq. (4) is equivalent to eq. (1), with additional nomenclature. Note that *BIF* is not a constant but varies according to the ratio G_{rear}/G_{POA}.

Substituting G_{eff} for G_{POA} in performance metrics, such as capacity tests and performance ratios, allows familiar monofacial equations for these metrics to be adapted for bifacial systems. For example, the draft of IEC 61724-1 Ed. 2 substitutes the product $BIF \cdot G_{POA}$ for G_{POA} in equations for performance ratio to obtain bifacial adaptations.

More detailed methods are being developed for more advanced assessment beyond the performance ratio metric, such as proposed in [8]. These issues are under a very early stage of review for bifacial updates to IEC 61724-2 and 61724-3.

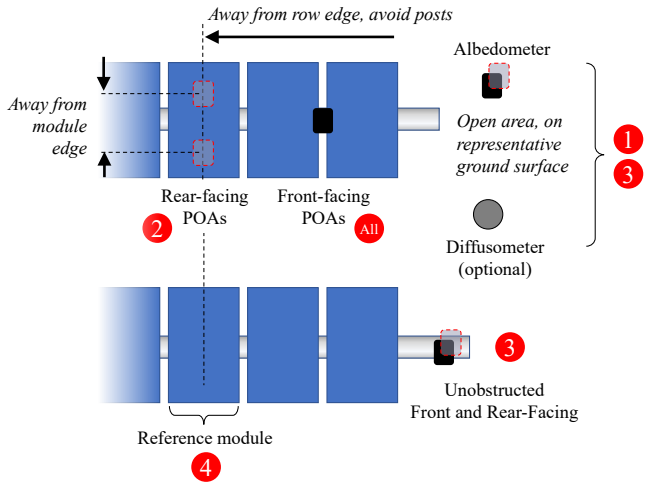


Fig. 9. Schematic options for irradiance sensor layout for approaches 1, 2, 3 and 4 discussed in section IV.

Although Eqs. (1)-(4) provide a way to express the combined effect of front and rear irradiance on system power output, to use these it is still necessary to determine values for G_{rear}. Various methods to obtain these data are discussed in the next section.

IV. Approaches to Irradiance Monitoring

Several different approaches to determining rear-side irradiance are being discussed in the research literature and international standards community while being pursued in practice on early systems. These different approaches address the challenges summarized in section II while making different tradeoffs. Here we review four approaches. Irradiance sensor placements for these approaches are schematically indicated in Fig. 9, while instrument options for them are listed in Table I together with potential advantages of different choices within each instrument category.

Approach 1: Modeling Rear-Side Irradiance

One approach, denoted "Option 1" in the draft of IEC 61724-1 Ed. 2, prescribes that the monitoring system should measure global horizontal irradiance (GHI), front-side POA, horizontal albedo and optionally also diffuse irradiance, and that these data are to be used with an optical model, such as a view-factor or ray-tracing model, to estimate the rear-side irradiance. The rear-side irradiance is then used in a performance model or in performance metrics via Eqs. (1)-(4).

One advantage of this approach is that it uses the optical model to deal with the complexities of rear-side irradiance non-uniformities – including within-module, within-row, and row-to-row uniformities – while keeping the measurement system relatively simple. The complexity of rear-side irradiance

uniformity can be handled at varying levels of detail depending on the model selection.

Furthermore, this approach allows measured irradiance and albedo data to be directly compared with pre-construction resource assessment data when comparing actual performance to design expectations.

However, since the approach relies on modeling to estimate rear-side irradiance, it does not provide any detailed information on the nature of possible deviations of the system from the model assumptions, which could be necessary for problem resolution as well as design validation and improvement. Furthermore, actual albedo may vary throughout the site due to differences in ground surface; therefore, albedometers should be placed above representative ground surfaces maintained identically to the ground surfaces underneath the modules.

Approach 2: Measuring Rear-Side Irradiance

"Option 2" in the draft of IEC 61724-1 Ed. 2 provides for directly measuring in-plane rear-side irradiance at multiple points distributed throughout the array, as shown in Fig. 9.

The relative advantages and disadvantages in comparison to "Option 1" discussed above are reversed. The rear-side irradiance (at the measurement points) is directly determined, allowing a precise comparison with design models and potentially greater confidence in assessing rear-side power contribution. In addition, measurement of rear irradiance at multiple points allows averaging over variations in ground surface throughout the site. However, rear-side irradiance cannot be directly compared to any pre-construction resource data. Also, non-uniformities in rear-side irradiance and variations in such non-uniformities make sensor placement critical.

Optimal positioning of rear-side irradiance sensors is not yet known. The draft of IEC 61724-1 Ed. 2 requires at least three rear-side irradiance measurement points per met station at the plant and instructs that these should be placed in representative locations throughout the plant and arranged to capture the effects of rear-side non-uniformity, while avoiding row-ends and unusual shading or reflections. However, the document does not prescribe specific locations of the sensors along the rear side. Guidance on this is evolving. Also, three rear-side measurement points are a minimum requirement in IEC 61724-1, with a greater number of measurement points frequently recommended.

For addressing non-uniformity along the module's width, [22] suggests locating the rear irradiance sensors along the module's collector width at 20% from the edges. This

TABLE I: MEASURED PARAMETERS AND INSTRUMENTS FOR EACH APPROACH IN SECTION IV

Approach	Measured Parameter	Instruments	Advantages	Notes
All	Global Horizontal Irradiance	• Broadband pyranometer	• Connection to satellite & historical resource data	
	Front-Facing Plane of Array Irradiance	• Reference cells	• Cost • Spectral, angular, time response matching PV modules	
1, 3	Albedo	• Broadband albedometers	• Connection to broadband tabulated albedo data, models	• Locate albedometers near the array with unobstructed view over similar ground type to the array
		• Reference cell albedometers	• Cost • Spectral match	
	Diffuse Horizontal Irradiance (optional)	• Tracked pyrheliometer or shaded pyranometer • Rotating shadow-band	• Accuracy	• Directly measure DHI, or measure DNI and GHI, from which DHI is calculated
		• Photodiode array with patterned shade • Reference cell array with varying orientations	• Cost	
2, 3, 4	Rear Irradiance	• Broadband pyranometers	• Many models predict broadband irradiance	• Avoid edge effects: 5m from row edges; 20% distance module edges • Avoid module shading by sensors • Keep sensors near module plane; avoid obstructions
		• Reference cells	• Cost • Spectral, angular, time response matching PV modules	
4	Effective Irradiance	• Bifacial reference module, measured at P_{max} (preferred) or I_{sc}	• Measure impact of non-uniform shading	• Directly measures effective irradiance, eq. (1)-(4)
All	Module Temperature	• Back-of-module temperature sensors		• Take care not to shade bifacial rear side; sensor and tapes must cover <10% of any cell's area

placement provides the most similar measurement to the single-value average rear irradiance models. To avoid edge effects, modeling has shown that a placement on center rows at least 5 meters from edges is ideal [23].

The large number of rear-side irradiance sensors required for this approach may favor the use of lower-cost irradiance sensors.

The ratio of co-located front and rear irradiance sensors has also been suggested for evaluating with more detail the real-time optical bifacial gains of a system [24].

Approach 3: Measuring Unobstructed Rear Irradiance

Since the non-uniformity of irradiance on the rear of the array with both time and position complicates the mapping of point measurements to the average rear-side irradiance, this approach intentionally moves the measurement location to the end of the tracker/row where measurements have fewer near-field obstructions. This option means the raw measurements are more stable but are biased relative to the spatially averaged rear irradiance available to the array, so the bias must be corrected for using a model. In practice, the model used for performance verification is adapted to produce estimates of the irradiance in this exposed location rather than averaged across the rear of the array, and the performance target is derived relative to this proxy measurement.

As depicted in Fig. 9, a rear-facing irradiance sensor located outboard from the rear of the array is exposed to a relatively unobstructed rear irradiance measurement. This is not physically representative of the light reaching the rear POA, but it is a stable location for measurement comparable with typical front-side POA measurements. It avoids impacts from diffuse shading on the array as well as the speckled, time-varying shade patterns that occur across the rear of the array even before structural shading is considered.

Since the irradiance components necessary to model average rear irradiance based on an unobstructed sensor reading are not easily available, use of this approach requires that the performance expectation be formulated relative to the unobstructed sensor rather than the modeled average input irradiance. On a fixed-tilt array modeled in PVsyst, the expected sensor input may be extracted by adding the structural obstruction term `BackShd` to the computed average irradiance reaching the surface `GlobBak`. For a horizontal north-south-axis single-axis tracker, a location that does not change height would be along the torque tube axis, and mounting at the equatorial end will minimize the amount of shade on the ground for the most stable measurements. The fractions of the field of view occupied by shaded and unshaded ground can be calculated and used to adapt the PVsyst intermediate rear irradiance components obtained using relevant (measured) ground albedo to predict the irradiance at the sensor location.

This approach combines the benefits of the two previously discussed approaches – while also requiring more irradiance sensors since both sets of measurements are performed. However, it minimizes the impact of measurement errors arising from rear-side time-varying shade patterns.

Approach 4: Bifacial Reference Devices

An alternative to separately measuring both front-side and rear-side in-plane irradiance is to use a bifacial reference device that simultaneously measures both quantities, as described in the draft of IEC 61724-1 Ed. 2. Such a bifacial reference device can be either a bifacial cell or a full-size bifacial module connected to an I-V measurement system. It should have identical response as the modules that are to be monitored, especially including identical bifaciality.

Bifacial reference cells, especially cells matched to a particular bifacial module, are not generally commercially available and must be supplied by the module manufacture.

Full-size bifacial modules identical to those in the array can be used, advantageously exactly matching module properties.

A significant benefit of using a bifacial reference module is that it intrinsically captures within-module rear-side irradiance non-uniformity, including shading effects that arise from the racking structure. If the module's power is measured, not just its short-circuit current, the result also provides the impact of irradiance non-uniformity on power production due to electrical mismatch.

With currently available in-field PV module I-V tracing units, use of a reference module takes up an otherwise productive slot in the array. However, automated I-V tracers that can isolate a single module from a string to measure an I-V curve and then switch back to regular operation are being developed and tested.

Due to the current lack of field calibration methods, bifacial reference modules may require calibration in a laboratory according to IEC 60904-1-2, and this step adds cost and logistical difficulties during construction, unless such modules are available as part of the due-diligence activities prior to construction.

A potential method for field calibration of a bifacial reference module comprises calibrating the module against a front-side POA reference cell while the module rear side is covered and using eq. (2) to determine a value for P_0. Subsequently, after uncovering the module rear side, module power P is used to measure effective irradiance G_{eff}. The rear-side contribution is estimated using the module bifaciality, which can be taken from the module datasheet or possibly determined by repeating the field calibration with the module mounted with its rear side facing front. Field calibration methods still require more development and validation.

V. Selecting an Approach

Selection of one of the measurement approaches described in section IV will depend on goals for uncertainty and cost as well as the user's application. Additionally, the user should

consider whether their objective is to measure only inputs (solar resource) and outputs (power), or also intermediate variables (rear-side irradiance).

The uncertainty of the measurement approach depends on both the instrumental uncertainty of the selected sensors and systematic uncertainties introduced by the many challenges discussed in section II. It is not yet possible to provide a general uncertainty estimate, but some examples are instructive. In one case analyzed by one of the authors, instrumental uncertainties involved in measuring rear-side irradiance on a single-axis tracking system were found to contribute 11.5% uncertainty in the predicted rear-side contribution, corresponding to ~2.3% uncertainty in total output; however, systematic uncertainties, for example arising from irradiance non-uniformity, were not estimated. Systematic uncertainties can be significant. In another case analyzed by one of the authors, a single-axis tracker system was found to produce almost 15% more energy than expected when the performance was predicted using only the overall incident solar resource and albedo data without measuring any rear irradiance quantities.

From these examples, we propose that the uncertainty of approach 1 in section IV, in which rear irradiance is not measured, should be considered greater than the uncertainty of approaches 2, 3, or 4.

The different approaches have different requirements for modeling. For system assessment relative to contractual performance guarantees, it is common to compare measured performance with expected performance for the measured conditions. For this purpose, it should be noted that approaches 1 and 3 require access to an irradiance model to estimate rear irradiance from other measured quantities, while approaches 2 and 4 can be used without an irradiance model since they directly measure the rear-side contributions. These factors may influence the selection of a measurement approach.

REFERENCES

[1] T. S. Liang *et al.*, "A review of crystalline silicon bifacial photovoltaic performance characterisation and simulation," *Energy and Environmental Science*, vol. 12, no. 1. Royal Society of Chemistry, pp. 116–148, Jan. 01, 2019, doi: 10.1039/c8ee02184h.

[2] C. W. Hansen *et al.*, "Analysis of irradiance models for bifacial PV modules," in *2017 IEEE 44th Photovoltaic Specialist Conference, PVSC 2017*, 2017, pp. 1–6, doi: 10.1109/PVSC.2017.8366322.

[3] C. Deline, S. Macalpine, B. Marion, F. Toor, A. Asgharzadeh, and J. S. Stein, "Assessment of Bifacial Photovoltaic Module Power Rating Methodologies-Inside and Out," *IEEE J. Photovoltaics*, vol. 7, no. 2, pp. 575–580, 2017, doi: 10.1109/JPHOTOV.2017.2650565.

[4] S. A. Pelaez, C. Deline, S. M. Macalpine, B. Marion, J. S. Stein, and R. K. Kostuk, "Comparison of Bifacial Solar Irradiance Model Predictions with Field Validation," *IEEE J. Photovoltaics*, vol. 9, no. 1, pp. 82–88, 2019, doi: 10.1109/JPHOTOV.2018.2877000.

[5] E. Ozkalay, J. Lopez-Garcia, L. Pinero-Prieto, A. Gracia-Amillo, and R. P. Kenny, "Evaluation of the non-uniformity of rear-side irradiance in outdoor mounted bifacial silicon PV modules," in *AIP Conference Proceedings*, Aug. 2019, vol. 2147, no. 1, p. 020011, doi: 10.1063/1.5123816.

[6] C. Monokroussos *et al.*, "Rear-side spectral irradiance at 1 sun and application to bifacial module power rating," *Prog. Photovoltaics Res. Appl.*, vol. 28, no. 8, pp. 755–766, Aug. 2020, doi: 10.1002/pip.3268.

[7] M. Waters, C. A. Deline, J. Kemnitz, and J. Webber, "Suggested Modifications for Bifacial Capacity Testing," in *2019 IEEE 46th Photovoltaic Specialists Conference (PVSC)*, 2019, pp. 3519–3524, doi: 10.1109/PVSC40753.2019.9198974.

[8] B. Marion, "Ground Albedo Measurements and Modeling Bill Marion 2018 Bifacial PV Workshop • Publication number or conference," 2018, Accessed: Mar. 23, 2021. [Online]. Available: https://pubs.er.usgs.gov/publication/ds1035.

[9] B. Marion, "Albedo from satellite and ground-based observations," 2019.

[10] G. Maclaurin, M. Sengupta, Y. Xie, and N. Gilroy, "Development of a MODIS-Derived Surface Albedo Data Set: An Improved Model Input for Processing the NSRDB," 2016, Accessed: May 10, 2021. [Online]. Available: https://www.osti.gov/biblio/1335471.

[11] M. Sengupta, Y. Xie, A. Lopez, A. Habte, G. Maclaurin, and J. Shelby, "The National Solar Radiation Data Base (NSRDB)," *Renewable and Sustainable Energy Reviews*, vol. 89. Elsevier Ltd, pp. 51–60, Jun. 01, 2018, doi: 10.1016/j.rser.2018.03.003.

[12] M. Sengupta, A. Habte, S. Wilbert, C. Gueymard, and J. Remund, "Best Practices Handbook for the Collection and Use of Solar Resource Data for Solar Energy Applications: Third Edition," Golden, CO (United States), Apr. 2021. doi: 10.2172/1778700.

[13] "Albedo (1 month) | NASA," May 2021.

[14] B. Marion, "Measured and satellite-derived albedo data for estimating bifacial photovoltaic system performance," *Sol. Energy*, vol. 215, pp. 321–327, Feb. 2021, doi: 10.1016/j.solener.2020.12.050.

[15] M. T. Patel, M. Ryyan Khan, A. Alnuaimi, O. Albadwawwi, J. J. John, and M. A. Alam, "Implications of Seasonal and Spatial Albedo Variation on the Energy Output of Bifacial Solar Farms: A Global Perspective," in *Conference Record of the IEEE Photovoltaic Specialists Conference*, Jun. 2019, pp. 2264–2267, doi: 10.1109/PVSC40753.2019.8981163.

[16] R. Bailey, P. Keelin, R. Perez, J. Robinson, G. Bender, and J. Chard, "Investigations of Site-Specific, Long Term Average Albedo Determination for Accurate Bifacial System Energy Modeling," in *Conference Record of the IEEE Photovoltaic Specialists Conference*, Jun. 2019, pp. 2268–2274, doi: 10.1109/PVSC40753.2019.8980744.

[17] T. C. R. Russell, R. Saive, A. Augusto, S. G. Bowden, and H. A. Atwater, "The Influence of Spectral Albedo on Bifacial Solar Cells: A Theoretical and Experimental Study," *IEEE J. Photovoltaics*, vol. 7, no. 6, pp. 1611–1618, 2017, doi: 10.1109/JPHOTOV.2017.2756068.

[18] S. Ayala Pelaez *et al.*, "Ultimate bifacial showdown: 75kW field results," in *7th bifiPV (virtual)*, 2020, pp. 1–35.

[19] M. Gostein, B. Marion, and B. Stueve, "Spectral Effects in Albedo and Rearside Irradiance Measurement for Bifacial Performance Estimation," in *2020 47th IEEE Photovoltaic Specialists Conference (PVSC)*, Jan. 2020, pp. 0515–0519, doi: 10.1109/pvsc45281.2020.9300518.

[20] M. Monarch and S. Ayala Pelaez, "Analysis and Validation of Spectral Irradiance Simulations for Methodology Results Conclusion and Future Work," *(in progress)*.

[21] A. Onno *et al.*, "Predicted Power Output of Silicon-Based Bifacial Tandem Photovoltaic Systems Predicted Power Output of Silicon-Based Bifacial Tandem Photovoltaic Systems," *Joule*, pp. 1–17, doi: 10.1016/j.joule.2019.12.017.

[22] S. Ayala Pelaez, C. Deline, J. S. Stein, B. Marion, K. Anderson, and M. Muller, "Effect of torque-tube parameters on rear-irradiance and rear-shading loss for bifacial PV performance on single-axis tracking systems," 2019.

[23] S. Ayala Pelaez, C. Deline, P. Greenberg, J. S. Stein, and R. K. Kostuk, "Model and validation of single-axis tracking with bifacial PV," *IEEE J. Photovoltaics*, vol. 9, no. 3, pp. 715–721, 2019, doi: 10.1109/JPHOTOV.2019.2892872.

[24] S. Ayala Pelaez *et al.*, "Field-Array Benchmark of Commercial Bifacial PV Technologies with Publicly Available Data," in *47th IEEE PVSC Proceedings*, 2020, pp. 1757–1759, doi: 10.1109/PVSC45281.2020.9300379.

View publication stats